https://doi.org/10.7840/kics.2024.49.12.1729

Spectral Efficient Frequency Division Multiplexing Aided with Tri-Mode Index Modulation in Mutli-Input Multi-Output Channels

Md. Shahriar Kamal◆, Muhammad Sajid Sarwar*, Soo Young Shin°

ABSTRACT

This work presents spectral efficient frequency division multiplexing with tri-mode index modulation (TM-SEFDM) for multi-input multi-output (MIMO) wireless networks. In TM-SEFDM, a fraction of subcarriers are utilized for modulation with two differentiable constellation sets, while the rest remains inactive. This strategy enables the transmission of extra bits through the subcarrier indices that correspond to the activation pattern of two constellation alphabets. Spectral efficiency (SE) and bit error rate (BER) are used to investigate the system's performance. The proposed MIMO-TM-SEFDM performs comparatively better than the conventional MIMO-SEFDM and MIMO-SEFDM with index modulation in SE and can achieve similar SE as MIMO dual-mode SEFDM analytically while being more energy efficient than DM. Both theoretic and numerical results for the MIMO-TM-SEFDM show improved error performance compared to the MIMO-SEFDM-IM system.

Key Words : Index modulation, multi-input multi-output, spectral efficient frequency division multiplexing, tri-mode

Ⅰ. Introduction

To accommodate rapidly increasing demand for data rates and massive connectivity, future wireless generation demands high spectral efficiency (SE). Multiinput multi-output (MIMO) is a promising technique for the ever-increasing user demands in the upcoming wireless generation. Orthogonal frequency division multiplexing (OFDM) has been used in wireless communications, but the thirst for higher SE is continuing. The purpose of deploying frequency domain index modulation, also known as subcarrier index modulation (IM), on OFDM is to design a spectral and energy efficient technique. Contrary to conventional OFDM, OFDM-IM does not activate all the available subcarriers; rather, it activates subcarriers partially based on an activation pattern to transmit supplemental information implicitly with no requirement of extra energy for transmission[1]. Hence, information can be conveyed in two ways; the indices of active subcarriers and the M-ary modulation on the active subcarriers[2]. Arbitrary grouping of subcarriers for OFDM-IM can result in performance gain in terms of achievable rate[3]. To achieve better error performance, lower order constellations with rotation are utilized where more bits are transmitted through subcarrier indices[4]. However, the partial inactivation inherited from conventional IM leads to inefficient us-

※ This work was supported by the National Research Foundation of Korea(NRF) grant funded by the Korea government. (MSIT) (No.2022R1A2B5B01001994, 50%). This research was also supported by the MSIT(Ministry of Science and ICT), Korea, under the ITRC(Information Technology Research Center) support program(IITP-2024-RS-2024-00437190, 50%) supervised by the IITP(Institute for Information Communications Technology Planning Evaluation).

◆ First Author : Kumoh National Institute of Technology, Department of IT Convergence Engineering, msrkamal@kumoh.ac.kr, 학생회원

° Corresponding Author : Kumoh National Institute of Technology, Department of IT Convergence Engineering, wdragon@kumoh.ac.kr, 종신회원

* Kumoh National Institute of Technology, Department of IT Convergence Engineering, sajid.sarwar@kumoh.ac.kr

논문번호 : 202407-126-B-RN, Received June 29, 2024; Revised July 29, 2024; Accepted August 10, 2024

age of frequency resources[1-3]. To utilize frequency resources efficiently dual mode (DM) OFDM makes use of all the available subcarriers. In addition to the diversity gain from the IM activation pattern DM-OFDM takes the help of two distinguishable constellation alphabets[1,5]. One mode to modulate subcarriers as per the activation pattern and another to modulate the remaining subcarriers. Unlike DM-OFDM, in generalized DM-OFDM (GDM-OFDM), the number of subcarriers to be modulated by either of the modes is flexible, enabling a comparatively higher number of possible realizations. This results in a better SE with a bit-error rate (BER) trade-off[6]. Multiple-mode OFDM-IM (MM-OFDM-IM) also utilizes all the subcarriers for OFDM systems through which multiple different constellations (or distinguishable modes) are transmitted to increase the SE[1,7].

Spectral efficient frequency division multiplexing (SEFDM) is a technique that compromises the OFDM through compression of subcarrier spacing to gain high SE at the expense of intercarrier interference (ICI)[8,9]. This technique is formulated from faster than Nyquist (FTN)[10,11], where symbols are packed in a nonorthogonal manner within the time domain; thereby violating the orthogonality criteria of Nyquist among the symbols[12]. Employing IM on SEFDM can mitigate ICI and improve BER performance[13,14]. A combination of OFDM and SEFDM with IM can further increase the overall data rate[15]. SEFDM-IM is also explored for MIMO channels to achieve energy efficiency (EE) with reduced ICI[16]. Though it provides high energy efficiency, it fails to achieve an SE higher than SEFDM because of partially inactive subcarriers[13,16,17]. Therefore, similar to the DM-OFDM case mentioned above, DM-SEFDM is proposed to use the frequency resources efficiently with the help of differentiable distinct constellation modes[17]. Although this can achieve high SE, it is not enegry efficient and could increase ICI due to the utilization of all non-orthogonal subcarriers of SEFDM.

Against the aforementioned background, tri-mode (TM) SEFDM for MIMO channels (MIMO-TM-SEFDM) is proposed to achieve SE gain and transmis-sion diversity. Unlike DM-SEFDM, subcarriers are activated partially to be modulated by two distinguishable constellation modes, which lowers the energy usage. With such an arrangement, the activation pattern can further carry extra information bits. As the index information in TM-SEFDM is higher than that of DM-SEFDM, TM makes up for the SE despite only a fraction of subcarriers being activated. The proposed MIMO-TM-SEFDM can mitigate ICI and can enable a balanced trade-off between BER and SE, while maintaining EE.

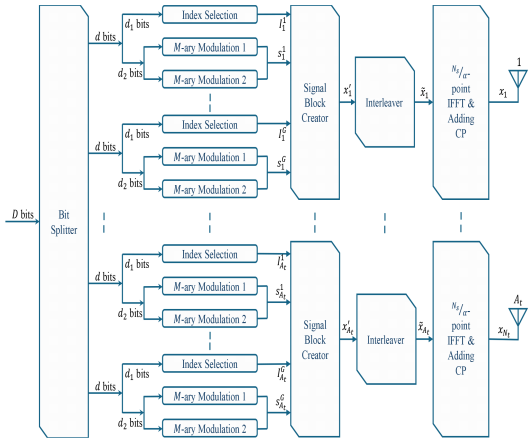

Fig. 1. Block diagram for MIMO-TM-SEFDM.

Ⅱ. System Model

The incoming D bits are factored for G groups. A total of DA_t bits are carried by this system. Since $D = dG$, every single group handles d bits. These groups are further utilized to transmit the SEFDM signal subblock of length $n = \frac{N_s}{G}$. The incoming bits for each group is $d = d_1 + d_2$, where d_1 bits determine the activation pattern of the subcarriers. Each of the subcarrier index is defined by I_a^g, where $a = \{1, 2, \cdots, A_t\}$ and $g = \{1, 2, \cdots, G\}$. In each group, from n subcarriers $k(= k_1 + k_2)$ are activated; where k_1 and k_2 carry the remaining bits d_2 through M_1 and M_2 constellation, respectively. The rest of the $n - k$ subcarriers are set to zero which helps to mitigate ICI among the nonorthogonal subcarriers of SEFDM system. The modulated symbols in the g^{th} group are indicated as s_a^g. After organizing the bits for respective depiction,the system has $d_1 = \left\lfloor \log_2 \binom{n}{k} \binom{k}{k_1} \right\rfloor$ as index bits and $d_2 = k_1 \log_2 M_1 + k_2 \log_2 M_2$ as modulation bits.

The transmission rate (bps/Hz) for the corresponding subblock can be expressed as follows.

$$C_g = \frac{1}{\alpha n}\left(\left\lfloor \log_2 \binom{n}{k}\binom{k}{k_1} \right\rfloor + k_1 \log_2 M_1 + k_2 \log_2 M_2\right), \quad (1)$$

where n indicates the g^{th} group's total number of subcarriers and α denote bandwidth compression factor. An example of subcarriers activation pattern of the proposed TM-SEFDM is presented in Table 1, where s_1 and s_2 are random elements of M_1 and M_2. The constellations M_1 and M_2 are differentiable and do not have any common points i.e., $M_1 \cap M_2 = \phi$. Considering classical M-ary phase shift keying (PSK) constellation for M_1 and M_2, a minimum distance of detachment between the adjacent signal points of these two modes needs to be equal or larger than least Euclidean distance of separation ($2sin(\frac{\pi}{M})$). This is achieved through the rotation of signal constellations of either M_1 or M_2. If $M_1 > M_2$ or $M_1 = M_2$, then rotation is applied to M_2. For example, when $M_1 = M$-PSK; $M_2 = \exp(\frac{\pi j}{M}) \times M$-PSK. In case $M_1 < M_2$, then the mode generation is done reversibly as $M_2 = M$-PSK and $M_1 = \exp(\frac{\pi j}{M}) \times M$-PSK, else the two modes can take similar points. The subcarriers' indices can be expressed as

$$\boldsymbol{i}_a^g = [i_a^g(1), i_a^g(2) \cdots i_a^g(k)]^{\mathrm{T}}. \quad (2)$$

Furthermore, the chosen indices are modulated using M-ary modulation to map d_2 bits and corresponding symbols are written as

$$\boldsymbol{s}_a^g = [s_a^g(1)\, s_a^g(2) \cdots s_a^g(k)]^{\mathrm{T}}, \quad (3)$$

where $s_a^g \in M_1$ and M_2 for k_1 and k_2 subcarriers, respectively. The remainder of the subcarriers ($n-k$) are set at zero value. This facilitates reduced ICI with EE for signal transmission. The signal from the g^{th} group through the a^{th} antenna is represented as

$$\hat{\boldsymbol{x}}_a^g = \left[\hat{x}_a^g(1)\, \hat{x}_a^g(2) \cdots \hat{x}_t^g(n)\right]^{\mathrm{T}} \quad (4)$$

where $\hat{x}_a^g(n)$ is denoted as follows

$$x_a^g(n) = \begin{cases} \boldsymbol{s}_a^g(k), & k \in \boldsymbol{i}_a^k \\ 0, & k \notin \boldsymbol{i}_a^g \end{cases} \quad (5)$$

An activation patter, known both at the transmitter and receiver, is considered using a look-up table (LUT) for small values of n and k. However, when the values are higher, combinatorial number theory is applied. These can be looked in detail from literature[1].

Groups are connected at each transmitter branch to create a block denoted as

$$\boldsymbol{x}_a' = \left[x_a'(1)\, x_a'(2) \cdots x_a'(N_s)\right]^{\mathrm{T}} = \left[(\hat{\boldsymbol{x}}_a^1)^{\mathrm{T}}\, (\hat{\boldsymbol{x}}_a^2)^{\mathrm{T}} \cdots (\hat{\boldsymbol{x}}_a^G)^{\mathrm{T}}\right]^{\mathrm{T}}, \quad (6)$$

and it can be expanded as

Table 1. A look-up table example ($k_1 = 1$, $k = 2$, $n = 4$, and $d_1 = 3$)

Data bits	Indices	TM-SEFDM sub-blocks
0 0 0	1, 2	[s1 , s2 , 0, 0]
0 0 1	2, 1	[s2 , s1 , 0, 0]
0 1 0	2, 3	[0, s1 , s2 , 0]
0 1 1	3, 2	[0, s2 , s1 , 0]
1 0 0	3, 4	[0, 0, s1 , s2]
1 0 1	4, 3	[0, 0, s2 , s1]
1 1 0	1, 4	[s1 , 0, 0, s2]
1 1 1	4, 1	[s2 , 0, 0, s1]

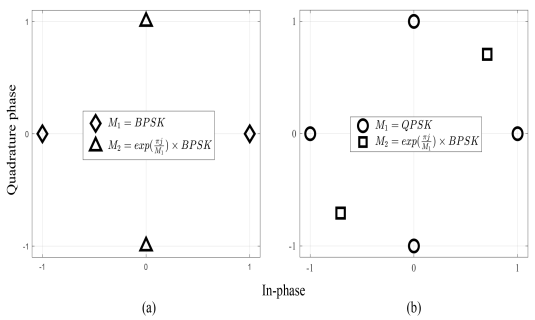

Fig. 2. Examples of constellations ensuring $M_1 \cap M_2 = \phi$ for (a) $M_1 = M_2$ = BPSK and (b) M_1 = QPSK, M_2 = BPSK.

$$\boldsymbol{x}_a' = [\hat{x}_a^1(1), \cdots \hat{x}_a^1(n), \hat{x}_a^2(1), \cdots \hat{x}_a^2(n), \cdots \hat{x}_a^G(1), \cdots \hat{x}_a^G(n)]^{\mathrm{T}} \quad (7)$$

Since the significant correlation between channel coefficients among the subcarriers within a group can be of an issue, subcarriers are spaced apart in the frequency domain through interleaving to obtain distinct fading. Interleaved arrangement of subcarriers incorporates frequency diversity and enhances the Euclidean distance among the symbols that are received. After being fed to a subcarrier-level interleaver, the vector in (7) gives the following output.

$$\tilde{\boldsymbol{x}}_a = [\hat{x}_a^1(1), \hat{x}_a^2(1), \ldots, \hat{x}_a^G(1), \ldots, \hat{x}_a^1(n), \hat{x}_a^2(n), \ldots, \hat{x}_a^G(n)]^T \quad (8)$$

For each of the SEFDM subblock, an inverse fast Fourier transform (IFFT) of size n/α is taken to generate non-orthogonal subcarriers based on the concept of decreased subcarrier spacing. To accommodate a larger number of subcarriers within the same bandwidth, a smaller subcarrier spacing than conventional OFDM is considered in SEFDM. This is done by choosing a bandwidth compression factor as $0 < \alpha < 1 (\alpha = \Delta f T)$. The frequency domain's minimum subcarrier spacing is denoted by Δf, whereas the time domain's symbol period is represented by T. However, α is 1 for conventional OFDM system. Partial deactivation of the subcarriers can lower the elevated ICI caused by SEFDM's subcarrier spacing, which is lower than the inverse of the symbol interval. Fig. 3 illustrates SEFDM cases for various modes of IM. The compression of subcarriers in SEFDM compared to OFDM is shown in the first two sub-figures, allowing incorporation of additional subcarriers within the same bandwidth. Then the partial activatoin of subcarriers based on the activation pattern in SEFDM-IM is shown in the third sub-figure. The next sub-figure presents that in DM-SEFDM, the subcarriers out of the activation pattern are also utilized a differentiable constellation alphabet (drawn in red). Lastly, subcarriers are partially activated in TM-SEFDM and uses two distinct constellation alphabets (differentiated by black and red) which further adds to the index bits. The integrated block of MIMO-TM-SEFDM signal can be represented as

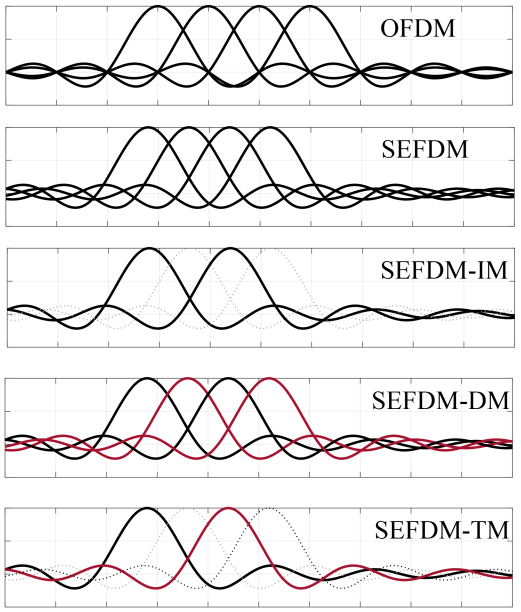

Fig. 3. Comparative subcarrier activation of differnt schemes.

$$\boldsymbol{x}_t = \frac{1}{\sqrt{T}} \sum_{i=0}^{N_s-1} \tilde{\boldsymbol{x}}_a \exp(j2\pi n \alpha t / T) \quad (9)$$

Nonetheless, the IFFT method normalizes the time-domain symbols to ensure that the expected total energy $E\{\boldsymbol{x}_a^{\mathrm{H}} \boldsymbol{x}_a\}$ equals N_s for all values of a. Then, to mitigate inter-symbol interference (ISI) a cyclic prefix (CP) is added at the start of the signal frame of every transmitter branch. Transmission of the resulting signal blocks is done from A_t antennas simultaneously over a MIMO channel that undergoes frequency selective Rayleigh fading $\boldsymbol{H}_{b,a} = \mathrm{ifft}\{\boldsymbol{G}_{b,a}\}$, where $b = 1, 2, \cdots, A_r$. Here, $\boldsymbol{G}_{b,a}$ represents the multi-path fading channel that varies with time. It is designed as a channel impulse response $\boldsymbol{G}_{b,a} = [G_{b,a}(1), \cdots, G_{b,a}(L)]^T$ between the transmitting antenna a and the receiving antenna b, where L denotes the number of channel taps. It is considered that each element of $\boldsymbol{G}_{b,a}$ is independent and identically distributed (i.i.d.) with $\mathcal{CN}(0, 1/L)$ and CP is greater than L. It is further assumed that during the transmission of a frame

the wireless chan-nel remains constant.

At the receiving end, the CP is removed from the received data blocks followed by which FFT is applied. A deinterleaver is employed at the receiving end to retrieve the interleaved signal from the transmitting side; hence, for interleaved as well as localized arrangement of subcarriers the same level of system complexity. Now, the signal received can be represented as:

$$\mathbf{y}_b = \sum_{a=1}^{A_t} \mathrm{diag}(\boldsymbol{x}_a)\boldsymbol{H}_{b,a} + \boldsymbol{w}_b, \tag{10}$$

where $\boldsymbol{y}_b = [y_b(1)\ y_b(2)\ \cdots\ y_b(N_s)]^{\mathrm{T}}$ is the received signal vector for the b^{th} antenna and $\boldsymbol{H}_{b,a} \in \mathbb{C}^{N_s \times 1}$ denotes wireless channel following $\mathcal{CN}(0,\ 1)$ distribution. Likewise, the noise vector in (11) defined by $\mathbf{w}_b \in \mathbb{C}^{N_s \times 1}$ is assumed to follow the $\mathcal{CN}(0,\ N_{0,F})$ distribution, where $N_{0,F}$ denotes the noise variance in frequency domain. This is associated with its time-domain equivalent and can be represented as $N_{0,F} = (\frac{k}{n})N_{0,T}$. Before detection, $\boldsymbol{y}_b$ can be segregated as follows.

$$\begin{aligned}
\boldsymbol{y}_b &= \left[\left(\boldsymbol{y}_b^1\right)^{\mathrm{T}} \left(\boldsymbol{y}_b^2\right)^{\mathrm{T}} \cdots \left(\boldsymbol{y}_b^G\right)^{\mathrm{T}}\right]^{\mathrm{T}} \\
\boldsymbol{x}_a &= \left[\left(\boldsymbol{x}_a^1\right)^{\mathrm{T}} \left(\boldsymbol{x}_a^2\right)^{\mathrm{T}} \cdots \left(\boldsymbol{x}_a^G\right)^{\mathrm{T}}\right]^{\mathrm{T}} \\
\boldsymbol{H}_{b,a} &= \left[\left(\boldsymbol{H}_{b,a}^1\right)^{\mathrm{T}} \left(\boldsymbol{H}_{b,a}^2\right)^{\mathrm{T}} \cdots \left(\boldsymbol{H}_{b,a}^G\right)^{\mathrm{T}}\right]^{\mathrm{T}} \\
\boldsymbol{w}_b &= \left[\left(\boldsymbol{w}_b^1\right)^{\mathrm{T}} \left(\boldsymbol{w}_b^2\right)^{\mathrm{T}} \cdots \left(\boldsymbol{w}_b^G\right)^{\mathrm{T}}\right]^{\mathrm{T}}.
\end{aligned} \tag{11}$$

For each group, the following representation can be derived from (11). $\overset{=}{}_{b,a}$

$$\boldsymbol{y}_b^g = \sum_{a=1}^{A_t} \mathrm{diag}(\boldsymbol{x}_a^g)\boldsymbol{H}_{b,a}^g + \boldsymbol{w}_b^g, \tag{12}$$

where $\boldsymbol{y}_b^g = \left[y_b^g(1) y_b^g(2) \cdots y_b^g(n)\right]^{\mathrm{T}}$ is the received signal vector at the b_{th} antenna that complies with the transmission vector $\boldsymbol{x}_a^g = \left[x_a^g(1) x_a^g(2) \cdots x_a^g(n)\right]^{\mathrm{T}}$. Additionally, the channel and noise vectors relating to that can be represented as $\boldsymbol{H}_{b,a}^g = \left[H_{b,a}^g(1)\, H_{b,a}^g(2) \cdots H_{b,a}^g(n)\right]^{\mathrm{T}}$ and $\boldsymbol{w}_b^g = \left[w_b^g(1)\, w_b^g(2) \cdots w_b^g(n)\right]^{\mathrm{T}}$, respectively.

For time-varying and frequency-selective channels, single-tap equalization is utilized in MIMO-OFDM system. However, with MIMO-SEFDM, as the bandwidth compression causes self-produced ICI it is difficult to apply. The channel state information (CSI) is supposed to be ideally derived through the transmission of pilots prior to data transmission. The ML based estimation of signal symbols for g^{th} group can be expressed as follows:

$$\left(\boldsymbol{x}_1^g, \ldots, \boldsymbol{x}_a^g\right)_{\mathrm{ML}} = \arg \min_{\left(\boldsymbol{x}_1^g, \ldots, \boldsymbol{x}_T^g\right)} \sum_{b=1}^{A_r} \left\| \boldsymbol{y}_r^g - \sum_{a=1}^{A_t} \mathrm{diag}(\boldsymbol{x}_a^g)\boldsymbol{H}_{b,a}^g \right\|^2 \tag{13}$$

To detect the index pattern and constellation symbol, a joint search for all of the transmitting antennas is conducted. Since each subblock is encoded independently, the signals are estimated subblock by subblock. The decoder searches for all possible combinations of index and symbols; therefore, complexity depends on the size of the LUT, which depends upon M and k. Hence, the order of complexity for the proposed MIMO-TM-SEFDM can be expressed as $O(M^{kA_t})$. On the contrary, for MIMO-DM-SEFDM, the order of complexity is $O(M^{nA_t})$, which is higher than MIMO-TM-SEFDM. Practical channel conditions can be explored by considering the effect of channel estimation errors by substituting $\boldsymbol{H}_{b,a}^g$ with $\tilde{\boldsymbol{H}}_{b,a}^g$ (least squares method estimation) in (13). Here, $\tilde{\boldsymbol{H}}_{b,a}^g = \boldsymbol{H}_{b,a}^g + \boldsymbol{e}^g$ and $\mathbf{e}^g$ is the estimationerror that has no dependency on $\boldsymbol{H}_{b,a}^g$.

Ⅲ. Performance Evaluation

3.1 Theoretical Bit Error Probability

In a case where $\boldsymbol{x}_a$ is transmitted and then the receiver erroneously decodes it as $\hat{\boldsymbol{x}}_a$, can result in decision errors on the M-ary constellation symbols as well as the active sub-carrier indices. The conditional pairwise error probability (PEP) for a single block is

$$\Pr\left(\boldsymbol{x}_a \to \hat{\boldsymbol{x}}_a \mid \tilde{\boldsymbol{H}}_{b,a}\right) \le Q\left(\sqrt{\frac{\left\|(\boldsymbol{x}_a - \hat{\boldsymbol{x}}_a)\tilde{\boldsymbol{H}}_{b,a}\right\|^2}{2\sigma_e^2}}\right), \tag{14}$$

where $\left\|(\boldsymbol{x}_a - \hat{\boldsymbol{x}}_a)\tilde{\boldsymbol{H}}_{b,a}\right\|^2 = (\tilde{\boldsymbol{H}}_{b,a})^H \boldsymbol{S}\, \tilde{\boldsymbol{H}}_{b,a}$, and $\boldsymbol{S} = (\boldsymbol{x}_a - \hat{\boldsymbol{x}}_a)^H(\boldsymbol{x}_a - \hat{\boldsymbol{x}}_a)$. An approximate expression of Q-function $\left[Q(v) = \left(\frac{1}{\sqrt{2\pi}}\int_v^\infty \exp\left(-\left(\frac{v^2}{2}\right)\right)dv\right)\right]$ is generally acquired as an exponenetial expression $Q(v) \cong \frac{1}{12}e^{-\frac{v^2}{2}} + \frac{1}{4}e^{-\frac{2v^2}{3}}$ [18]. For the proposed MIMO-TM-SEFDM, analysis based on John W. Craig's formula is deployed[19]. The unconditional PEP is achieved by taking mean of the instantaneous channel states as follows:

$$\begin{aligned} P(\boldsymbol{x}_a \to \hat{\boldsymbol{x}}_a) &\cong \mathrm{E}_{\tilde{\boldsymbol{H}}_{b,a}}\left\{\frac{e^{-\frac{\varepsilon_S \delta}{4\sigma_e^2}}}{12} + \frac{e^{-\frac{\varepsilon_S \delta}{3\sigma_e^2}}}{4}\right\} \\ &\cong \frac{\frac{1}{12}}{\det(\mathbf{I}_n + q_1 \mathbf{C}_n \mathbf{S})} + \frac{\frac{1}{4}}{\det(\mathbf{I}_n + q_2 \mathbf{C}_n \mathbf{S})}, \end{aligned} \tag{15}$$

where $\mathbf{I}_n$ is an identity matrix, $\mathbf{C}_n = \mathrm{E}\{\tilde{\boldsymbol{H}}_{b,a}(\tilde{\boldsymbol{H}}_{b,a})^H\}$, $q_1 = 1/4\sigma_e^2$, and $q_2 = 1/3\sigma_e^2$. Thus, the analytical bit error probability can be expressed as

$$P_e \le \frac{1}{d\psi}\sum_{\boldsymbol{x}_a}\sum_{\hat{\boldsymbol{x}}_a} P(\boldsymbol{x}_a \to \hat{\mathbf{x}}_a) Z(\boldsymbol{x}_a, \hat{\boldsymbol{x}}_a) \tag{16}$$

where $d = d_1 + d_2$ is explained in the proposed system model above, $\psi = 2^d$, represent the number of probable realizations for the given user, and $Z(\boldsymbol{x}_a, \hat{\boldsymbol{x}}_a)$ is the number of bits that are in error (bits in $\hat{\boldsymbol{x}}_a$ that differs from $\boldsymbol{x}_a$).

3.2 Spectral Efficiency

The data rates of MIMO-TM-SEFDM, MIMO-DM- SEFDM, MIMO-SEFDM-IM, and MIMO-SEFDM can be derived as follows:

$$R_{TM} = \frac{1}{\alpha}\left(\left\lfloor \log_2\left(\binom{n}{k}\binom{k}{k_1}\right)\right\rfloor + k_1 \log_2 M_1 + k_2 \log_2 M_2\right) \tag{17}$$

$$R_{DM} = \frac{1}{\alpha}\left(\left\lfloor \log_2\binom{n}{k}\right\rfloor + k\log_2 \hat{M}_1 + (n-k)\log_2 \hat{M}_2\right) \tag{18}$$

$$R_{IM} = \frac{1}{\alpha}\left(\left\lfloor \log_2\binom{n}{k}\right\rfloor + k\log_2 M\right) \tag{19}$$

$$R_{SEFDM} = \frac{1}{\alpha}\left(n\log_2 \hat{M}\right) \tag{20}$$

where M_1 and M_2 are the modulation order in MIMO-TM-SEFDM; $\hat{M}_1$ and $\hat{M}_2$ are the modulation order in MIMO-DM-SEFDM. M and $\hat{M}$ are the modulation sizes in MIMO-SEFDM-IM and MIMO-SEFDM, respectively. The total number of data bits that can be transmitted per group with respect to the number of activated subcarriers is presented in Fig. 4. The following are the parameters in Fig. 4 for each group of subcarriers ($n = 4$ subcarriers in one group). SEFDM: $\hat{M}$ = *BPSK* modulation with all n subcarriers; SEFDM-IM: k active subcarriers in each group, M = *BPSK* modulation with the k active subcarriers; DM-SEFDM: k chosen subcarriers based on the index modulation pattern, $\hat{M}_1$ = *BPSK* modulation with k subcarriers, while $\hat{M}_2$ = *BPSK* modulation with $n - k$ subcarriers; TM-SEFDM: k active subcarriers in each group, M_1 = *BPSK* modulation with k_1 activated subcarriers and M_2 = *BPSK* modulation with $k_2 (= k - k_1)$

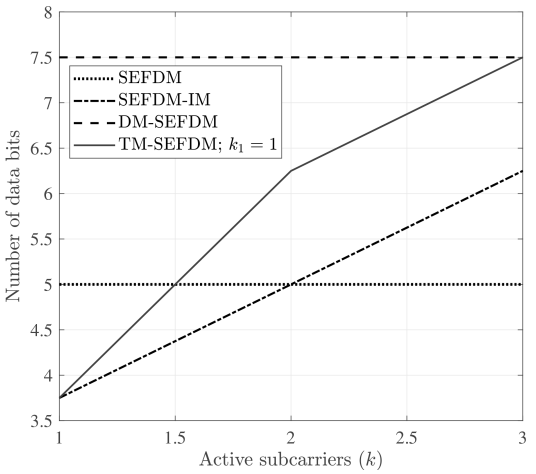

Fig. 4. Comparison of data rate per group.

activated subcarriers; the compression factor $\alpha = 0.8$ for all the schemes. The proposed MIMO-TM-SEFDM is observed to achieve a higher data rate per group compared to the conventional MIMO-SEFDM and MIMO-SEFDM-IM. Moreover, the same data rate as MIMO- DM-SEFDM can be achieved at $k = 3$ by the proposed scheme while being energy efficient due to the partial activation of subcarriers. This is possible as the index bits with TM-SEFDM are higher than with DM-SEFDM.

3.3 Energy Efficiency

The EE of the proposed MIMO-TM-SEFDM in comparison with MIMO-DM-SEFDM can be calculated follows.

$$\eta = \frac{\xi_{TM-SEFDM} - \xi_{DM-SEFDM}}{\xi_{DM-SEFDM}} \times 100\% = \frac{(k_1 \log_2 M_1 + k_2 \log_2 M_2) - (k \log_2 \hat{M}_1 + (n-k) \log_2 \hat{M}_2)}{k \log_2 \hat{M}_1 + (n-k) \log_2 \hat{M}_2} \times 100\% = \left(\frac{k_1 \log_2 M_1 + k_2 \log_2 M_2}{k \log_2 \hat{M}_1 + (n-k) \log_2 \hat{M}_2} - 1 \right) \times 100\%,$$

where ξ is the normalized energy. Considering fixed values of α(= 0.85), n(= 4), and k(= 2) the EE can be measured using the above expression. When $\hat{M}_1 = \hat{M}_2 = 2$ in DM-SEFDM, approximately 7 bits are transmitted per group of subcarriers. To achieve the same SE, TM-SEFDM with $k_1 = k_2 = 1$ can use $M_1 = 4$ and $M_2 = 2$. Hence, the EE in this case, $\eta = -25\%$. However, for fixed values of α, n, and k, comparatively larger M_1 and/or M_2 are required for large values of $\hat{M}_1$ and/or $\hat{M}_2$ to gain the same SE. This declines the EE gain of TM-SEFDM. For example, when $\hat{M}_1 = 32$ and $\hat{M}_2 = 4$ in DM-SEFDM, $M_1 = 32$ and $M_2 = 64$ in TM-SEFDM, resulting in $\eta \approx -8.33\%$.

Ⅳ. Result Discussion

The performance of the proposed MIMO-TM-OFDM is investigated and compared with other index modulated SEFDM schemes under frequency-selective Rayleigh fading channel. In simulations, the number of subcarriers N_s, the CP length, and the length of channel fading coefficients L are set to 64, 16, and 10, respectively. For each of the schemes, a total of 16 groups are considered; therefore, each group consists of 4 subcarriers.

In Fig. 5, the BER performance of the proposed system is compared against the existing MIMO-DM-SEFDM and MIMO-SEFDM-IM to achieve a data rate of 6 bits per group. Different subcarrier compression is required for TM, IM, and DM to achieve the same data rate per group. The legend is interpreted as: TM: $(4, 2, 1, BPSK) \rightarrow n = 4, k = 2, k_1 = 1, M_1 = M_2$ = BPSK; DM: $(4, 2, BPSK) \rightarrow n = 4, k = 2, M_1 = M_2$ = BPSK; IM: $(4, 2, BPSK) \rightarrow n = 4, k = 2, M =$ BPSK. For each of the schemes, cases with and without interleaved subcarrier grouping are considered. In both cases, the BER performance of MIMO-TM-SEFDM is almost the same as that of MIMO-DM-SEFDM and better than that of MIMO-SEFDM-IM. Also, every scheme performs better with interleaved grouping than with regular subcarrier grouping. A gain of 2 dB is observed for TM with interleaving at BER 1.25×10^{-4} compared to that with local grouping. Frequency diversity and the Euclidean distance enhancement among the received symbols through interleaving contribute to the performance gain. Additionally the numerical BER of the proposed scheme is validated through the theoretical BER analysis. With n, k, and M parameters fixed, as MIMO-DM-SEFDM utilizes all the subcarriers, the

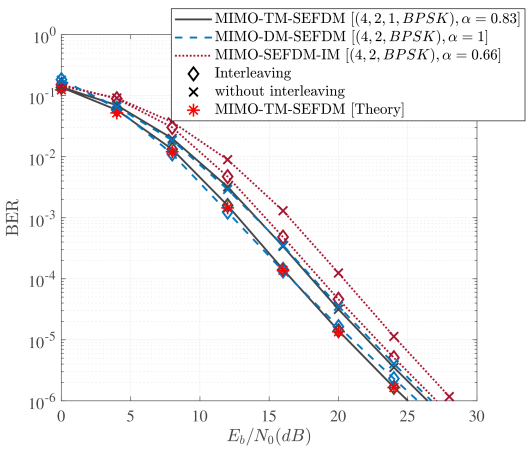

Fig. 5. BER comparison of the proposed MIMO-TM-SEFDM with MIMO-SEFDM-IM and MIMO-DM-SEFDM (MIMO order 2 × 2).

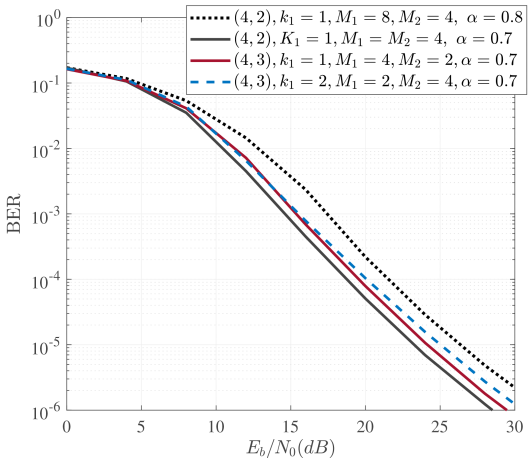

Fig. 6. BER comparison of MIMO-TM-SEFDM for different configurations (MIMO order 2 × 2).

same data rate is achieved without compressing the subcarrier spacing. Whereas, a low compression of subcarriers (17%) is needed for MIMO-TM-SEFDM due to the partial activation of the subcarriers. However, the same error performance is observed for MIMO-TM-SEFDM as for MIMO-DM-SEFDM, while MIMO-TM-SEFDM is energy efficient. Fig. 6 illustrates the error performance of MIMO-TM-SEFDM with varying configurations to achieve the same data rate per group of 10 bits. In cases where 3 subcarriers are activated in a group, it is observed that variation of the values of k_1, M_1, and M_2 results in a similar BER curve. On the contrary, for the cases with 2 active subcarriers, 3 *dB* gain is achieved with lower modulation (M_1 = M_2 = QPSK) and more compression (30%) over the one with higher modulation (M_1 = 8-PSK, M_2 = QPSK) and less compression (20%) to reach BER of 5.1×10^{-5}. Hence, a comparatively lower order of modulation with correspondingly less compression can be preferred for the proposed scheme.

V. Conclusions

In this paper, MIMO-TM-SEFDM is proposed to improve the BER performance and SE of existing index modulated SEFDM schemes. Only a portion of subcarriers in each SEFDM group are modulated by two distinctly identifiable constellation modes, which add extra information on top of the index pattern through the subcarrier indices. This ensures EE with a balance between SE and BER. The proposed MIMO-TM-OFDM surpasses conventional MIMO-SEFDM-IM and matches MIMO-DM-SEFDM in terms of SE and BER.

References

[1] T. Mao, Q. Wang, Z. Wang, and S. Chen, "Novel index modulation techniques: A survey," *IEEE Commun. Surv. Tuts.*, vol. 21, no. 1, pp. 315-348, 2019. (https://doi.org/10.1109/COMST.2018.2858567)

[2] E. Başar, Ü. Aygölü, E. Panayırcı, and H. V. Poor, "Orthogonal frequency division multiplexing with index modulation," *IEEE Tran. Signal Process.*, vol. 61, no. 22, pp. 5536-5549, 2013. (https://doi.org/10.1109/TSP.2013.2279771)

[3] M. Wen, X. Cheng, M. Ma, B. Jiao, and H. V. Poor, "On the achievable rate of OFDM with index modulation," *IEEE Trans. Signal Process.*, vol. 64, no. 8, pp. 1919-1932, 2016. (https://doi.org/10.1109/TSP.2015.2500880)

[4] S. A. Nambi and K. Giridhar, "Lower order modulation aided BER reduction in OFDM with index modulation," *IEEE Commun. Lett.*, vol. 22, no. 8, pp. 1596-1599, 2018. (https://doi.org/10.1109/LCOMM.2018.2844355)

[5] T. Mao, Z. Wang, Q. Wang, S. Chen, and L. Hanzo, "Dual-mode index modulation aided OFDM," *IEEE Access*, vol. 5, pp. 50-60, 2017. (https://doi.org/10.1109/ACCESS.2016.2601648)

[6] T. Mao, Q. Wang, and Z. Wang, "Generalized dual-mode index modulation aided OFDM," *IEEE Commun. Lett.*, vol. 21, no. 4, pp. 761-764, 2017. (https://doi.org/10.1109/LCOMM.2016.2635634)

[7] M. Wen, E. Basar, Q. Li, B. Zheng, and M.

Zhang, “Multiple-mode orthogonal frequency division multiplexing with index modulation,” *IEEE Trans. Commun.*, vol. 65, no. 9, pp. 3892-3906, 2017. (https://doi.org/10.1109/TCOMM.2017.2710312)

[8] N. H. Nguyen, H. H. Nguyen, and B. Berscheid, “SVD-based design for non-orthogonal frequency division multiplexing,” *IEEE Commun. Lett.*, vol. 25, no. 4, pp. 1343-1347, 2021. (https://doi.org/10.1109/LCOMM.2020.3045719)

[9] M. Jia, Z. Yin, Q. Guo, G. Liu, and X. Gu, “Downlink design for spectrum efficient IoT network,” *IEEE Internet of Things J.*, vol. 5, no. 5, pp. 3397-3404, 2018. (https://doi.org/10.1109/JIOT.2017.2734815)

[10] I. Darwazeh, H. Ghannam, and T. Xu, “The first 15 years of SEFDM: A brief survey,” in *2018 11th Int. Symp. Commun. Syst., Netw. Digital Signal Processing* (*CSNDSP*), pp. 1-7, 2018. (https://doi.org/10.1109/ CSNDSP.2018.8471886)

[11] T. Xu and I. Darwazeh, “Non-orthogonal narrowband internet of things: A design for saving bandwidth and doubling the number of connected devices,” *IEEE Internet of Things J.*, vol. 5, no. 3, pp. 2120-2129, 2018. (https://doi.org/10.1109/JIOT.2018.2825098)

[12] T. Xu and I. Darwazeh, “Transmission experiment of bandwidth compressed carrier aggregation in a realistic fading channel,” *IEEE Trans. Veh. Technol.*, vol. 66, no. 5, pp. 4087-4097, 2017. (https://doi.org/10.1109/TVT.2016.2607523)

[13] M. Nakao and S. Sugiura, “Spectrally efficient frequency division multiplexing with indexmodulated non-orthogonal subcarriers,” *IEEE Wireless Commun. Lett.*, vol. 8, no. 1, pp. 233-236, 2019. (https://doi.org/10.1109/LWC.2018.2867869)

[14] Y. Chen, T. Xu, and I. Darwazeh, “Index modulation pattern design for non-orthogonal multicarrier signal waveforms,” *IEEE Trans. Wireless Commun.*, vol. 21, no. 10, pp. 8507-8521, 2022. (https://doi.org/10.1109/TWC.2022.3166850)

[15] M. S. Sarwar and S. Y. Shin, “SEFDM based index modulation on OFDM-IM,” *IEEE Wireless Commun. Lett.*, vol. 12, no. 11, pp. 1906-1910, 2023. (https://doi.org/10.1109/LWC.2023.3298918)

[16] M. S. Sarwar, M. Ahmad, and S. Y. Shin, “Subcarrier index modulation for spectral efficient frequency division multiplexing in multi-input multi-output channels,” *IEEE Trans. Veh. Technol.*, vol. 72, no. 2, pp. 2678-2683, 2023. (https://doi.org/10.1109/TVT.2022.3213011)

[17] M. S. Sarwar, I. N. A. Ramatryana, M. Ahmad, and S. Y. Shin, “Dual-mode index modulation for non-orthogonal frequency division multiplexing,” *IEEE Trans. Wireless Commun.*, vol. 22, no. 11, pp. 7712-7726, 2023. (https://doi.org/10.1109/TWC.2023.3254558)

[18] M. Chiani, D. Dardari, and M. Simon, “New exponential bounds and approximations for the computation of error probability in fading channels,” *IEEE Trans. Wireless Commun.*, vol. 2, no. 4, pp. 840-845, 2003. (https://doi.org/10.1109/TWC.2003.814350)

[19] S. Dang, G. Ma, B. Shihada, and M.-S. Alouini, “A novel error performance analysis methodology for OFDM-IM,” *IEEE Wireless Commun. Lett.*, vol. 8, no. 3, pp. 897-900, 2019. (https://doi.org/10.1109/LWC.2019.2899091)

Md. Shahriar Kamal

Feb. 2019 : BSc. in Engg., University of Chittagong, Bangladesh.

Sep. 2022-Current : MS. student, Kumoh National Institute of Technology, South Korea.

<Research Interest> 5G/6G wireless communications and networks, multi-input multioutput networks, multiple access techniques, etc.

[ORCID:0000-0002-0109-661X]

Muhammad Sajid Sarwar

Aug. 2016 : BSc. Eng., University of Engineering & Technology, Lahore.

Mar. 2017-Aug. 2019 : MS. Engg., COMSATS University, Islamabad, Lahore Campus.

Mar. 2021-Aug. 2024 : Ph.D., Kumoh National Institute of Technology.

<Research Interest> Non-orthogonal frequency division multiplexing techniques, multi-input multi-output wireless networks, non-orthogonal multiple access, orbital angular momentum communications, and random access techniques.

[ORCID:0000-0002-4584-7702]

Soo Young Shin

Feb. 1999 : B.Engg. degree, School of Electrical and Electronic Engineering, Seoul National University.

Feb. 2001 : M.Engg. degree, School of Electrical, Seoul National University.

Feb. 2006 : Ph.D. degree, School of Electrical Engineering and Computer Science, Seoul National University.

July 2006-June 2007 : Post Doc. Researcher, School of Electrical Engineering, University of Washington, Seattle, USA.

2007-2010 : Senior Researcher, WiMAX Design Laboratory, Samsung Electronics, Suwon, South Korea.

Sept. 2010-Current : Professor, School of Electronic Engineering, Kumoh National Institute of Technology.

<Research Interest> 5G/6G wireless communications and networks, signal processing, the Internet of Things, mixed reality, and drone applications.

[ORCID:0000-0002-2526-2395]